Corneal Biomechanical Changes and Tissue Remodeling After SMILE and LASIK

Rohit Shetty,[1] Mathew Francis,[2] Rushad Shroff,[1] Natasha Pahuja,[1] Pooja Khamar,[1] Molleti Girrish,[2] Rudy M. M. A. Nuijts,[3] and Abhijit Sinha Roy[2]

[1]Cornea and Refractive Surgery Division, Narayana Nethralaya, Bommansandra, Bangalore, India
[2]Imaging, Biomechanics and Mathematical Modeling Solutions (IBMS) Lab, Narayana Nethralaya Foundation, Bangalore, India
[3]Department of Ophthalmology, University Hospital Maastricht, The Netherlands

Correspondence: Abhijit Sinha Roy, Narayana Nethralaya Foundation, #258A Hosur Road, Bommansandra, Bangalore, India; asroy27@yahoo.com.

Submitted: August 24, 2017
Accepted: October 11, 2017

Citation: Shetty R, Francis M, Shroff R, et al. Corneal biomechanical changes and tissue remodeling after SMILE and LASIK. *Invest Ophthalmol Vis Sci*. 2017;58:5703–5712. DOI:10.1167/iovs.17-22864

Purpose. To evaluate transient corneal tissue healing and biomechanical changes between laser in situ keratomileusis (LASIK) and small incision lenticule extraction (SMILE) eyes.

Methods. In each patient, one eye underwent LASIK and the other underwent SMILE. Optical coherence tomography (OCT) and dynamic Scheimpflug imaging (Corvis-ST) was used to assess tissue healing and biomechanics, respectively. Analyses of OCT scans yielded corneal speckle distribution (CSD) and Bowman's roughness index (BRI). Waveform analyses of deformation amplitude yielded corneal stiffness. Further, corneal force versus corneal deformation data helped compare the two procedures.

Results. BRI increased and then decreased transiently after both treatments ($P < 0.05$). However, SMILE eyes had BRI similar to that of their preoperative state compared to LASIK eyes at 6-month follow-up. CSD indicated a marked increase in the number of bright pixels and a decrease in the number of dark pixels after SMILE (1-month follow-up) and LASIK eyes (3-month follow-up), respectively. CSD returned to near preoperative state thereafter, respectively. Corneal stiffness change from preoperative state was similar between LASIK and SMILE eyes. However, deformation at discrete values of corneal force indicated some recovery of biomechanical strength after SMILE, but not in LASIK eyes.

Conclusions. BRI and CSD indicated earlier tissue healing in SMILE eyes than in LASIK. CSD results may indicate delayed cell death in LASIK eyes and increased light scatter due to interface fluid in SMILE eyes. Corneal biomechanical strength remodeled better in SMILE. This may indicate some hydration-related recovery.

Keywords: corneal biomechanics, SMILE, LASIK, optical coherence tomography

First reports of small incision lenticule extraction (SMILE) refractive surgery came in the year 2011.[1,2] The true implication of absence of a laser-assisted in situ keratomileusis (LASIK) flap in SMILE has been a subject of intense study. There were several clinical studies on biomechanical changes in the cornea after LASIK and SMILE.[3–10] A few reported similar biomechanical changes in the cornea after femtosecond LASIK and SMILE.[3–6] Other studies reported better biomechanical outcomes in SMILE eyes than in LASIK eyes.[7–10] Similarly, corneal tissue healing and Scheimpflug densitometry changes indicated a moderately better response in SMILE eyes.[11–13] These studies highlighted the need for improved analyses of information derived from current clinical devices to compare LASIK and SMILE outcomes.

Speckle distribution in optical coherence tomography (OCT) images of the cornea could assist in quantification of tissue-level changes in patients.[14–16] The earlier studies used a probability distribution function (pdf) to describe the speckle distribution and then analyzed the change in pdf parameters as biomarkers of tissue response.[15,16] The OCT images were also a great source of corneal structural data. Micro-distortions in the Bowman's layer after SMILE indicated transient remodeling of the cornea.[17] We have developed the Bowman's roughness index (BRI) to quantitatively map the micro-distortions after refractive surgery and in disease, for example, keratoconus.[18,19] BRI indicated thinning of the Bowman's layer in keratoconus.[18] However, BRI indicated the presence of a small amount of micro-distortions naturally before SMILE surgery that underwent a transient increase followed by decrease in magnitude postoperatively.[19] Since these tissue morphologic changes occurred due to the surgery, these could also contribute to biomechanical changes in the cornea as ectasia may occur due to poor preoperative or lower residual biomechanical properties of the cornea.[20] Current in vivo biomechanical assessment options are the Corvis-ST (Oculus Optikgeräte GmbH, Wetzlar, Germany) and the Ocular Response Analyzer (ORA) (Reichert Ophthalmic Instruments, Buffalo, NY, USA). Both the devices are air-puff applanation devices. However, correlation between ORA indices and mechanical corneal stiffness is unknown.[21,22] Using Corvis-ST, we can derive corneal stiffness, specific to the in vivo corneal deformation amplitude waveform.[23] Quantitative corneal stiffness was reported in myopic eyes,[23,24] in keratoconic eyes before and after accelerated crosslinking,[25] and in eyes undergoing SMILE.[19] Therefore, the objectives of this study were (1) to quantitatively map the biophysical changes in the cornea using OCT speckle distribution and BRI and (2) to quantitatively map the change in corneal stiffness with Corvis-ST and relate it to biophysical changes. These

quantifications were performed before and after refractive surgery, where one eye of the patient underwent LASIK and the other eye underwent SMILE. Thus, the study design was contralateral.

Methods

The research study was longitudinal and prospective. The ethics committee of Narayana Nethralaya Multi-Specialty Eye Hospital, Bangalore, India, approved the study. The study followed the tenets of the Declaration of Helsinki. All participants provided written informed consent. The study included a total of 31 patients. One eye underwent SMILE while the other underwent LASIK. A random number generator assigned either SMILE or LASIK to an eye. Inclusion criteria were stable refraction (less than −10 diopter [D] equivalent refraction with astigmatism not more than −3 D) for a period of 1 year (change less than 0.25 D). Patients with less than 480-μm central corneal thickness (CCT) or history of keratoconus, diabetes, collagen vascular disease, pregnancy, breastfeeding, and any prior ocular surgery or trauma were excluded from the study. In all the eyes, calculated residual stromal thickness was greater than 250 μm. All patients underwent refractive error assessment (sphere, cylinder, and axis), Corvis-ST measurement, and high-resolution OCT imaging (Envisu; Leica Microsystems, Buffalo Grove, IL, USA). If the patients were contact lens users, then contact lens use was discontinued for at least 2 weeks before measurements. Corvis-ST measurements were performed preoperatively and at 1-, 3-, and 6-month follow-up. This was avoided at 1 week to avoid any patient discomfort. OCT imaging was performed preoperatively and 1 week, 1 month, and once between the 3- and 6-month follow-up periods. In our earlier study, OCT imaging had revealed near normalization of BRI by the 3-month follow-up in SMILE patients.[19] Therefore, OCT imaging was repeated only once between the 3- and 6-month follow-up periods to avoid unnecessary imaging.

Surgical Procedure

A single experienced surgeon performed all the surgeries under topical anesthesia using 0.5% proparacaine hydrochloride (Paracain; Sunways Pvt. Ltd., Mumbai, India) instilled two or three times. The WaveLight FS200 femtosecond laser and WaveLight EX500 excimer laser platform (Alcon Laboratories, Inc., Fort Worth, TX, USA) cut the flap and ablated the tissue in one eye. The flap had a 9.0-mm diameter, 110-μm thickness, a side cut angle of 70°, canal width of 1.5 mm, and hinge position at 90°. Optical zone diameter was 6.0 mm. Targeted refractive error treatment reshaped the cornea with excimer laser after manual lifting of the flap. The VisuMax femtosecond laser system (Carl Zeiss Meditec AG, Jena, Germany) cut the cap and lenticule in the fellow eye. Cap thickness was 110 μm. Lenticule and cap diameter was 6.0 and 7.7 mm, respectively. After creation of the refractive lenticule, it was dissected and extracted manually through a superior 3-mm side cut. Cornea was remoistened with a wet Merocel sponge at the end of the procedure. After the surgery, one drop of moxifloxacin hydrochloride 0.5% (Vigamox; Alcon Laboratories, Inc.) was applied to both eyes. Routine postoperative regimen was followed for both eyes. This included moxifloxacin hydrochloride 0.5% eye drops (Vigamox; Alcon Laboratories, Inc.) four times a day for 1 week, tapering doses of topical 1% fluorometholone eye drops (Flarex; Alcon Laboratories, Inc.), and topical lubricants (Optive; Allergan, Inc., Parsippany, NJ, USA) four times a day for 3 months.

Corneal Biomechanical Analyses

An analytical biomechanical model analyzed the deformation amplitude waveform from Corvis-ST.[23–25] The analyses yielded the corneal stiffness.[23–25] The model reported two measures of stiffness: a linear corneal stiffness [Kc (constant), unit N/m] and a mean corneal stiffness [Kc (mean), unit N/m].[23–25] In classical biomechanics, analyses of the ex vivo stress versus strain curves provided the tissue biomechanical properties. Therefore, we analyzed the air-pressure force absorbed by the cornea, named the corneal force, and the corneal deformation only.[23–25] Here, corneal force and corneal deformation were considered analogous to stress and strain, respectively. At each time point for a given eye, the data were regressed with a third-order polynomial equation. All regressions achieved a minimum $R^2 = 0.98$. At each time point, the equations for all the eyes were averaged to obtain the mean corneal force versus corneal deformation response for the two cohorts (LASIK and SMILE). Using the mean corneal force versus corneal deformation data, the mean corneal deformation at a mean corneal force of 0.10, 0.15, 0.20, and 0.25 N was calculated at each time point. These were compared between the treatment cohorts.

OCT Image Analyses

Analyses of the OCT images yielded BRI[18,19] and speckle distribution. BRI was a measure of roughness of the Bowman's layer.[18,19] Postoperatively, this roughness was expected to be higher in the acute healing phase after surgery.[19] To analyze the speckle distribution, only the raw OCT images were used. The scan size was limited to 3 mm in the high-resolution mode. The procedure to acquire the OCT images was discussed previously.[18] The Bioptigen InVivo Vue 2.2.22 reader software (Bioptigen, Inc., Morrisville, NC, USA) exported the raw images for further analyses. The aspect ratio of the exported images was maintained for the analyses. Preoperatively, the cornea had a healthy tear film. However, postoperative dryness, along the anterior surface, caused additional scattering in the total image. Therefore, the analyses of the speckle distribution were performed using two methods.

In the first method, a pdf, without any noise correction, mapped the speckle distribution. Figure 1a shows a grayscale representation of the uncorrected image. The image region within the anterior and posterior corneal edge was selected (Fig. 1b). The regions above (air) and below (aqueous humor) the cornea are shown in Figure 1c with pseudocoloring. The pdfs mapped the speckle distribution of air, cornea, and aqueous humor (Figs. 1d–f, respectively). Here, the pdf calculated for the uncorrected corneal image was the first method. This method was applied to both pre- and postoperative time points. In the second method, a corrected corneal image resulted from subtraction of the speckle distribution of the air and aqueous humor from the "whole image" speckle distribution (Figs. 1g, 1h in grayscale and pseudocoloring, respectively). The same pdf mapped the speckle distribution of corrected corneal image (Fig. 1i). From Figures 1g and 1h, it was evident that the air and aqueous humor had negligible speckle after correction. The second method was also applied to both pre- and postoperative states. Thus at any given time point, two pdfs for the cornea were calculated, one for the uncorrected and the other for the corrected OCT image.

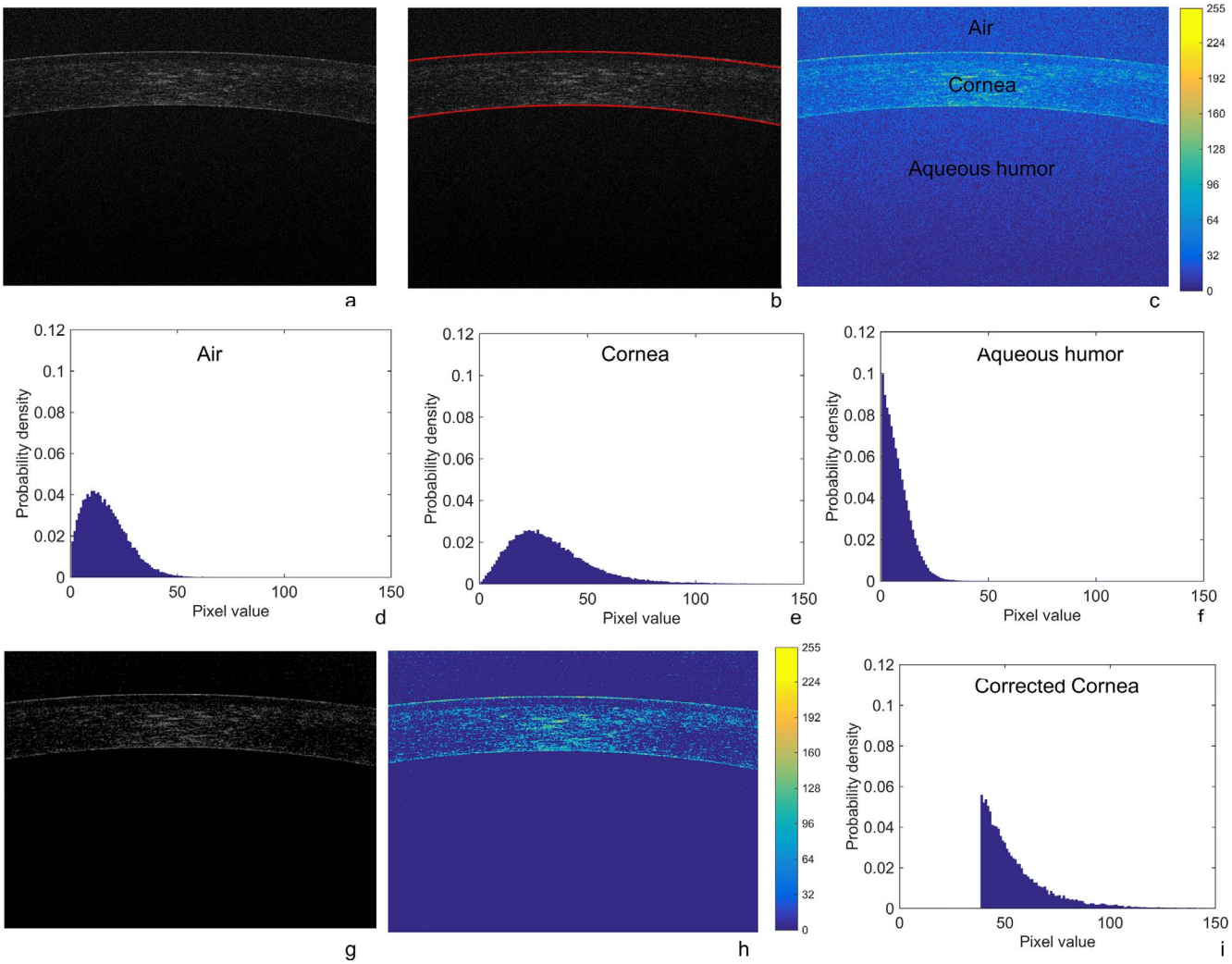

Figure 1. An OCT scan of the cornea without (**a**) and with (**b**) detected bounding edges. The same with pseudocolors is shown in (**c**), showing the air, cornea, and aqueous humor. (**d**–**f**) The speckle distribution of air, cornea, and aqueous humor regions, respectively. (**g**, **h**) The same image after correction and with pseudocoloring, respectively. (**i**) The corneal speckle distribution after image correction.

The generalized extreme value (GEV) pdf (Equation 1) captured the tails (i.e., speckle distribution at or near the highest intensity of 255) of different shapes accurately.[26] Pixel intensity ranged from 0 to 255 in the OCT images. Therefore, it was necessary to model both extremes of intensity with a suitable mathematic function. The GEV was a three-parameter function: μ ($-\infty \leq \mu \leq \infty$), σ ($\sigma \geq 0$), and k ($-\infty \leq k \leq \infty$). Here, these parameters represent location, scale, and shape, respectively.[26] The value of k described the shape of the distribution; for example, $k = 0$ represented the Gumbel distribution, $k > 0$ represented the Frechet distribution, and $k < 0$ represented the Weibull distribution. The tail of the pdf described the number of the pixels with higher intensity. The Gumbel distribution, also known as GEV type 1 distribution, described an exponentially decreasing tail better, similar to a normal distribution. The Weibull distribution (type 3) described a tail of finite length. The Frechet distribution (type 2) was suited for distributions with very small tails. Scale parameter (σ) influenced the maximum height of the pdf. When σ decreased, the number of high-intensity pixels decreased and low-intensity pixels increased. Location parameter (μ) influenced the location of the peak of the pdf along the x-axis of the distribution. If μ increased, the peak moved toward the highest intensity (pixel value of 255), and the converse held as well.

$$f(x) = \begin{cases} \frac{1}{\sigma}\left(1 + k\frac{(x-\mu)}{\sigma}\right)^{-1-\frac{1}{k}} e^{\left(-\left(1+k\frac{(x-\mu)}{\sigma}\right)^{-\frac{1}{k}}\right)} & \text{for } k \neq 0 \\ \frac{1}{\sigma} e^{\left(-e^{\left(-\frac{(x-\mu)}{\sigma}\right)}\right)} - \frac{(x-\mu)}{\sigma} & \text{for } k = 0 \end{cases} \quad (1)$$

The GEV distribution parameters (σ, k, μ) were computed using maximum likelihood estimation.[26] For each eye, three scans were acquired at each time point to assess repeatability of BRI,[18] σ, k, and μ. To analyze the difference between the cohorts of LASIK and SMILE eyes, the means of the GEV distribution parameters (σ, k, and μ) were used. These mean values yielded the mean speckle distributions for the LASIK and SMILE cohort at different time points.

The normality of the data was confirmed with Shapiro-Wilk test. Repeated measures analysis of variance (ANOVA) was used to study the change after the surgery in the LASIK and SMILE cohorts. Repeatability of the data was analyzed with intraclass correlation coefficient (ICC). The mean ± standard error of the parameters was calculated. A P value less than 0.05 was considered statistically significant. All statistical calcula-

Table 1. Optical Coherence Tomography (OCT) Speckle Parameters From Uncorrected and Corrected Corneal Images

	LASIK				SMILE					
	Preoperative	1 wk	1 mo	3 mo and Beyond	Preoperative	1 wk	1 mo	3 mo and Beyond	*P* Value LASIK	*P* Value SMILE
Corneal probability density function parameters from uncorrected image										
k	0.06 ± 0.02	0.07 ± 0.01	0.05 ± 0.01	0.08 ± 0.01	0.03 ± 0.01	0.05 ± 0.01	0.06 ± 0.01	0.04 ± 0.01	0.64	0.39
σ	14.37 ± 0.68	14.69 ± 0.82	13.22 ± 0.69	15.28 ± 0.92	14.3 ± 0.64	16.27 ± 0.92	14.47 ± 0.75	14.71 ± 0.91	0.30	0.33
μ	25.29 ± 1.44	25.8 ± 1.62	22.35 ± 1.1	24.28 ± 1.38	25.94 ± 1.43	28.92 ± 1.97	25.43 ± 1.55	26.15 ± 1.79	0.32	0.49
Corneal probability density function parameters from corrected image										
k	0.41 ± 0.02	0.42 ± 0.02	0.44 ± 0.02	0.44 ± 0.03	0.37 ± 0.02	0.37 ± 0.02	0.42 ± 0.02	0.4 ± 0.02	0.64	0.19
σ	8.72 ± 0.54	8.66 ± 0.52	7.44 ± 0.37	9.68 ± 0.64	8.36 ± 0.47	10.05 ± 0.65	8.21 ± 0.38	8.81 ± 0.68	0.03*	0.12
μ	45.73 ± 1.02	46.92 ± 1.41	43.36 ± 1.08	46.13 ± 1.44	44.82 ± 1.29	48.31 ± 1.50	45.06 ± 0.9	44.47 ± 1.19	0.23	0.12

* Indicates statistically significant difference.

tions were performed using MedCalc v17.6 software (MedCalc Software, Ostend, Belgium).

Results

The mean age of the patients was 24 ± 1 years. The manifest refraction spherical equivalent (MRSE) [–7.22 ± 1.32 and –6.18 ± 0.41 D for LASIK and SMILE, respectively; $P = 0.45$], intraocular pressure (IOP) [13.5 ± 0.46 and 13.0 ± 0.45 mm Hg for LASIK and SMILE, respectively; $P = 0.41$], and CCT [517 ± 4.89 and 514.18 ± 4.5 μm for LASIK and SMILE respectively; $P = 0.67$] were similar between the eyes. The ratio of female to male patients was 1.21 (17 female and 14 male patients). The ICC of BRI, k, σ, and μ for each zone (air, aqueous humor, and cornea) was greater than 0.95, indicating high repeatability. Table 1 shows the mean ± standard error of k, σ, and μ of the cornea, before and after correction. Most parameters (k, σ, and μ) were similar ($P > 0.05$) between the time points, irrespective of the procedure (LASIK or SMILE). In the corrected corneal image, only σ showed a significant temporal decrease in the LASIK eyes at 1 month ($P = 0.03$ in Table 1). In SMILE, an increase in σ was observed at 1 week after surgery, but this increase was not statistically significant. Since most parameters in Table 1 did not achieve statistical significance, we used the mean values of k, σ, and μ to plot the mean corneal speckle distributions for the LASIK and SMILE cohort eyes.

Using the uncorrected corneal images, Figures 2a and 2b show the mean distributions for LASIK and SMILE eyes, respectively. We focused on two regions of the distributions as shown in insets (Figs. 2a, 2b). Figures 2c and 2e show the magnified regions of the distributions plotted in Figure 2a (LASIK eyes). Figures 2d and 2f show the magnified regions of the distributions plotted in Figure 2b (SMILE eyes). In LASIK eyes (Fig. 2c), there was a sharp increase in peak of the distribution from preoperative (red line) to 1 month (blue line). At 3 months, the peak (purple line) reduced below the peak of the preoperative distribution (Fig. 2c). An increase in peak of the distribution logically would indicate more pixels in the high-intensity pixel range since the total number of pixels in each image was the same at all time points. This was evident in Figure 1e, where the number of pixels in the high-intensity regions was the least at 1 month (blue line). At other time points (Fig. 2e), the number of pixels was approximately the same [preoperatively (red line), 1 week (green line), and beyond 3 months (purple line)]. In SMILE eyes, a marked decrease in peak of the distribution (green line in Fig. 2d) and increase in the number of pixels in the high-intensity region (green line in Fig. 2f) at 1 week showed up postoperatively. Thereafter, the distributions at 1 month (blue line in Figs. 2d, 2f) and beyond 3 months (purple line in Figs. 2d, 2f) were similar to the preoperative distribution (red line in Figs. 2d, 2f). Interestingly, the corrected corneal images showed the same trends as well (Fig. 3). Thus, the speckle distribution indicated a longer-duration remodeling of the cornea in LASIK eyes than in SMILE eyes.

In LASIK eyes, mean BRI was $1.72 \times 10^{-3} \pm 1.31 \times 10^{-4}$, $4.49 \times 10^{-3} \pm 1.35 \times 10^{-4}$, $3.21 \times 10^{-3} \pm 1.27 \times 10^{-4}$, and $2.49 \times 10^{-3} \pm 1.18 \times 10^{-4}$ mm^2 preoperatively, 1 week, 1 month, and 3 months plus follow-up, respectively. Further, mean BRI differed significantly between all the time points when analyzed pairwise ($P = 0.001$). Interestingly, in LASIK eyes, mean BRI beyond 3 months was still greater than the preoperative magnitude. In SMILE eyes, BRI was $2.31 \times 10^{-3} \pm 1.29 \times 10^{-4}$, $4.52 \times 10^{-3} \pm 1.41 \times 10^{-4}$, $4.01 \times 10^{-3} \pm 1.29 \times 10^{-4}$, and $2.54 \times 10^{-3} \pm 1.18 \times 10^{-4}$ mm^2, respectively. In SMILE eyes, the trends were similar between the time points ($P = 0.001$) except between preoperative and 3 months plus follow-up ($P > 0.05$). In other words, BRI beyond 3 months had returned to preoperative magnitudes in most eyes. Thus, postoperative wound healing appeared to be better in SMILE eyes than in LASIK eyes.

Biomechanical analyses of the eyes yielded interesting results. In LASIK eyes, the kc (constant) was 103.87 ± 1.55, 92.37 ± 1.95, 93.67 ± 1.48, and 91.39 ± 2.41 N/m at preoperative, postoperative 1 month, postoperative 3 months, and postoperative 6 months, respectively. In SMILE eyes, the same was 102.75 ± 1.39, 90.02 ± 1.68, 92.14 ± 1.66, and 89.5 ± 2.09 N/m at preoperative, postoperative 1 month, postoperative 3 months, and postoperative 6 months, respectively. In LASIK eyes, kc (mean) was 101.8 ± 1.84, 85.85 ± 2, 86.23 ± 1.78, and 84.03 ± 2.29 N/m at preoperative, postoperative 1 month, postoperative 3 months, and postoperative 6 months, respectively. In SMILE eyes, the same was 100.37 ± 1.85, 83.04 ± 1.82, 83.41 ± 1.94, and 79.64 ± 2.09 N/m at preoperative, postoperative 1 month, postoperative 3 months, and postoperative 6 months, respectively. In LASIK eyes, there was a significant decrease in stiffness between pre- and postoperative states ($P < 0.001$), but not between the postoperative time points ($P > 0.05$). The SMILE eyes showed the same trends.

Since changes in stiffness parameters were similar between LASIK and SMILE, the mean values of derived biomechanical model parameters[23–25] yielded the mean corneal force versus corneal deformation curves at all time points. Figures 4a and 4b show these plots for LASIK and SMILE eyes. We evaluated these plots at discrete values of force, and the corresponding corneal deformation was derived from Figures 4a and 4b (Table 2). At a force of 0.10 and 0.15 N and in LASIK eyes, change (= preoperative − postoperative time point) in corneal deformation was similar at all postoperative time points (Table 2; $P =$

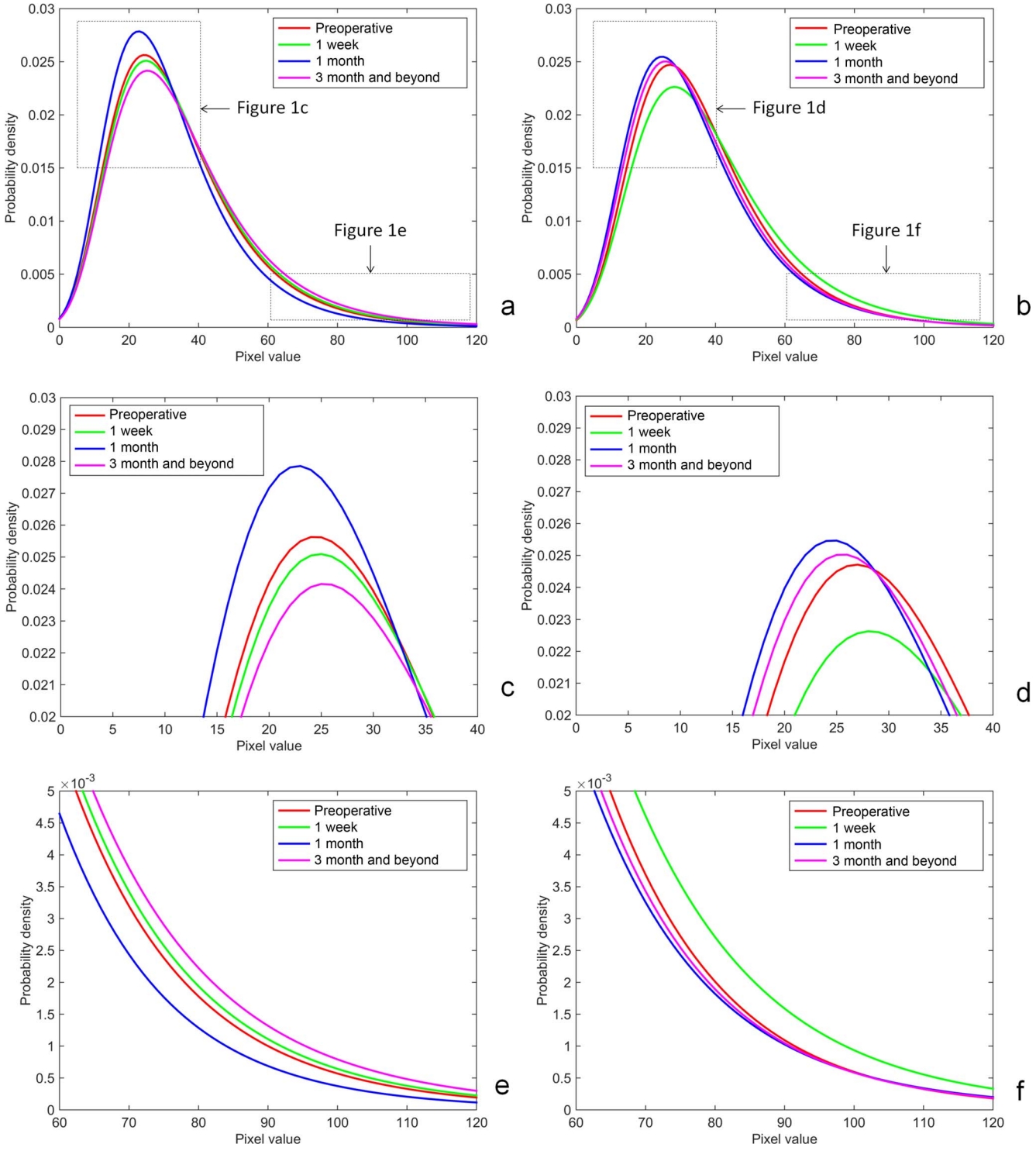

Figure 2. Uncorrected mean speckle probability distribution function (pdf) in LASIK (**a**) and SMILE (**b**) eyes. The magnified peak and tail section of LASIK (**c**, **e**, respectively) and SMILE (**d**, **f**, respectively) eyes are shown as well. Data for all time points are plotted.

0.71 and 0.47, respectively). The SMILE eyes showed the same trends (Table 2; $P = 0.47$ and 0.12, respectively). In LASIK eyes, the trend was the same at higher corneal forces of 0.20 and 0.25 N. However in SMILE eyes, there was a significant decrease in change in corneal deformation from 1 month (approximately –0.1 mm) to 6 months (approximately –0.022 mm). This could indicate a better remodeling of the collagen matrix in SMILE eyes than in LASIK eyes (similar to BRI). These results were also evident upon careful visual examination of Figures 4a and 4b.

Discussion

The cornea is a complex tissue, where a delicate balance between mechanical and fluid stresses determines its shape

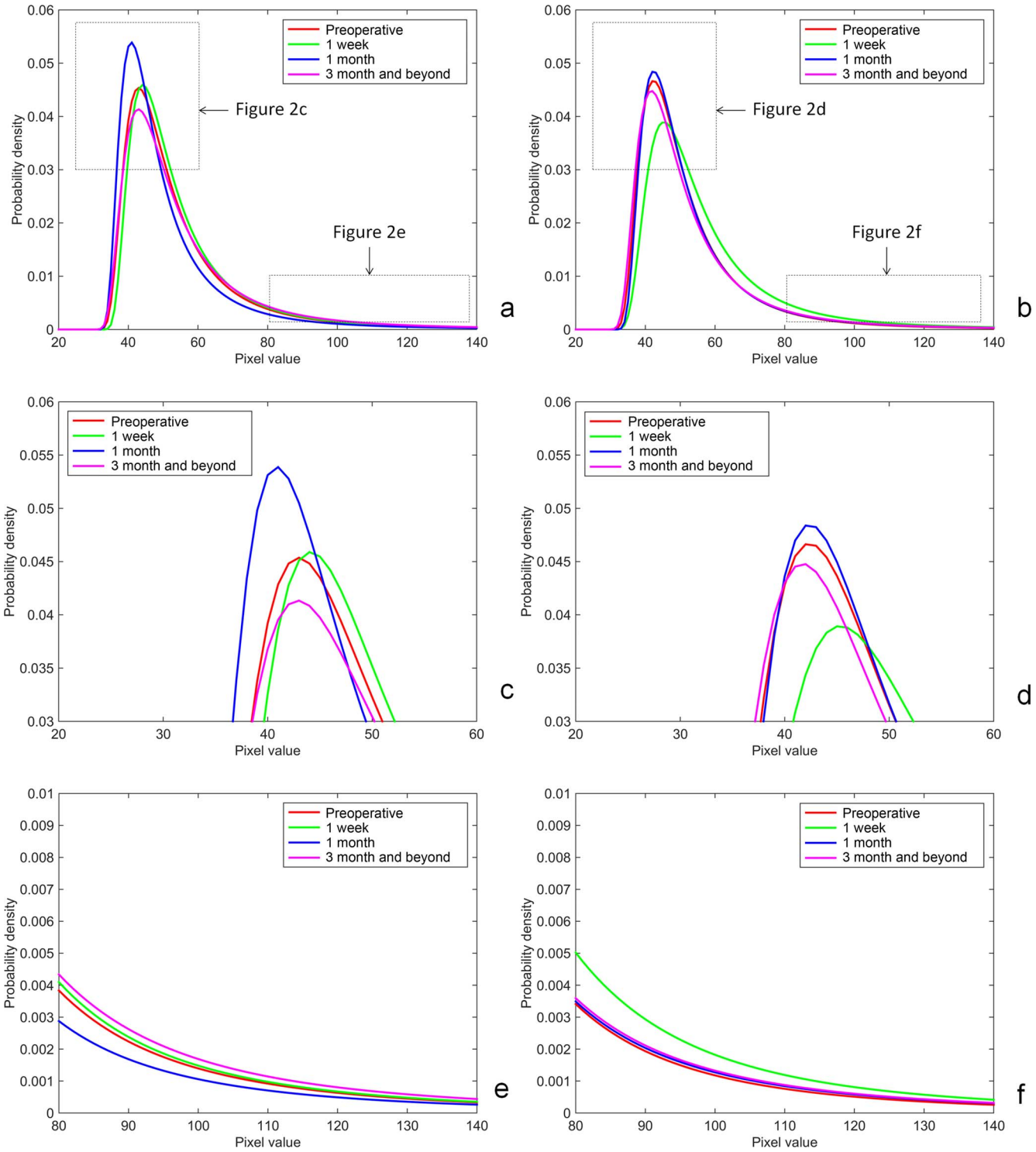

FIGURE 3. Corrected mean speckle probability distribution function (pdf) in LASIK (**a**) and SMILE (**b**) eyes. The magnified peak and tail section of LASIK (**c**, **e**, respectively) and SMILE (**d**, **f**, respectively) eyes are shown as well.

and function. This complexity impacts the transient wound healing and deformation response after LASIK and SMILE. We presented novel applications of OCT imaging biomarkers to assess tissue-level changes in the cornea. Based on BRI and corneal speckle distribution, both LASIK and SMILE caused structural changes. Figures 5a and 5b provide a schematic representation of the transient wound healing and biomechanical changes in SMILE and LASIK eyes, respectively. In SMILE eyes, postoperative corneal speckle changed up to 1 week and was nearly back to preoperative distribution by 1 month (Fig. 5a). In the case of BRI, the return to preoperative levels was achieved by the third month. However, corneal deformation continued to remodel up to the 6-month follow-up and possibly beyond (Fig. 5a). In LASIK eyes, corneal speckle normalized by the 3-month follow-up (Fig. 5b). However, BRI and corneal deformation possibly continued to remodel even

Table 2. Change (Preoperative Minus Postoperative) in Corneal Deformation Levels at Different Applied Corneal Force Computed Using the Analytical Biomechanical Model

Corneal Force	LASIK			SMILE			*P* Value LASIK	*P* Value SMILE
	1 mo, mm	3 mo, mm	6 mo, mm	1 mo, mm	3 mo, mm	6 mo, mm		
0.10 N	−0.07 ± 0.01	−0.06 ± 0.01	−0.06 ± 0.02	−0.1 ± 0.01	−0.08 ± 0.01	−0.08 ± 0.02	0.71	0.47
0.15 N	−0.06 ± 0.01	−0.04 ± 0.01	−0.04 ± 0.02	−0.08 ± 0.01	−0.06 ± 0.01	−0.04 ± 0.02	0.47	0.12
0.20 N	−0.07 ± 0.02	−0.05 ± 0.01	−0.04 ± 0.02	−0.09 ± 0.01	−0.05 ± 0.02	−0.022 ± 0.017	0.41	0.03*
0.25 N	−0.09 ± 0.02	−0.06 ± 0.02	−0.05 ± 0.02	−0.1 ± 0.02	−0.06 ± 0.02	−0.022 ± 0.021	0.43	0.03*

* Indicates statistically significant difference.

after the 6-month follow-up. This is the first study to present these interesting features of in vivo corneal wound healing and biomechanics.

A recent study used corneal densitometry from Scheimpflug imaging to analyze transient healing of the cornea after photorefractive keratectomy (PRK), LASIK, and SMILE.[12] The mean postoperative total corneal densitometry values were 15.53 ± 1.65, 16.53 ± 1.94, and 16.10 ± 1.54, respectively.[12] Thus, the procedures caused similar densitometry changes.[12] Scheimpflug imaging uses visible light for densitometry and has lower axial resolution compared to OCT. In contrast, LASIK and SMILE caused different structural responses in this study. This could be due to differences between infrared light and tissue interaction coupled with better axial resolution of OCT. BRI was another novel index to quantify the micro-distortions in the Bowman's layer.[18] BRI was greater after both SMILE and LASIK due to surgical manipulations in LASIK and compression of the cap in SMILE. Therefore, we hypothesized structural changes in the flap/cap region (Fig. 6).

Preoperatively (Fig. 6), the helical collagen fibers were under tension.[27] Under stress relaxation (due to surgical severance of collagen fibers), the fibers could undergo a crimping effect.[26] This is shown by the compression of the helical structure postoperatively (Fig. 6a). In other words, this could possibly lead to an increase in BRI (Fig. 6a). As the cornea remodeled further, the collagen fibers relaxed and possibly resulted in a lower BRI (Fig. 6b). In SMILE, only a small number of fibers in the cap were cut. This could explain the faster relaxation of the fibers in SMILE. However, LASIK severed a much larger number of fibers. This could have significantly delayed the return of BRI to preoperative levels. It would be interesting to study if BRI recovers after LASIK in the long term, similar to SMILE (Fig. 5). By design, SMILE was a less invasive procedure than LASIK. Therefore, it was logical to hypothesize a significant biomechanical advantage of SMILE over LASIK. Studies have reported mixed results on change in corneal biomechanical parameters after SMILE and LASIK.[3–10] A contralateral eye study on SMILE versus LASIK reported similar changes in CH and CRF between the eyes.[6] In this study as well, change in corneal stiffness was similar between the eyes. However, stiffness was an aggregate marker of the nonlinear stress versus strain response of the patient cornea.[23–25] Therefore, discrete locations on the mean corneal force versus corneal deformation curves (Fig. 4) were analyzed. At low corneal forces where the deformation response of the cornea may be linear, the change in deformation was barely different between the LASIK and SMILE eyes (Fig. 4). However, at higher forces, the SMILE corneas showed a clear trend toward some recovery of the biomechanical strength at follow-up (Fig. 4). Interestingly, at high forces, the collagen fibers bear some of the mechanical stress. This could be correlated to differences between SMILE and LASIK eyes with respect to transient changes in BRI.

Our analytical model revealed interesting results between myopic eyes from different populations.[23–25] In this study, transient changes in BRI, corneal speckle, and corneal deformation in SMILE eyes indicated a strong interdependence between these corneal properties; for example, BRI and cornea speckle returned to preoperative levels by the third month and coupled with transient changes in corneal deformation in SMILE eyes. In LASIK, this was not observed. Thus, flap and excimer ablation in LASIK could have caused these observations. Excimer ablation may result in greater hydration changes. Transient decrease in number of high-intensity pixels could indicate greater (detectable by OCT) keratocyte death in

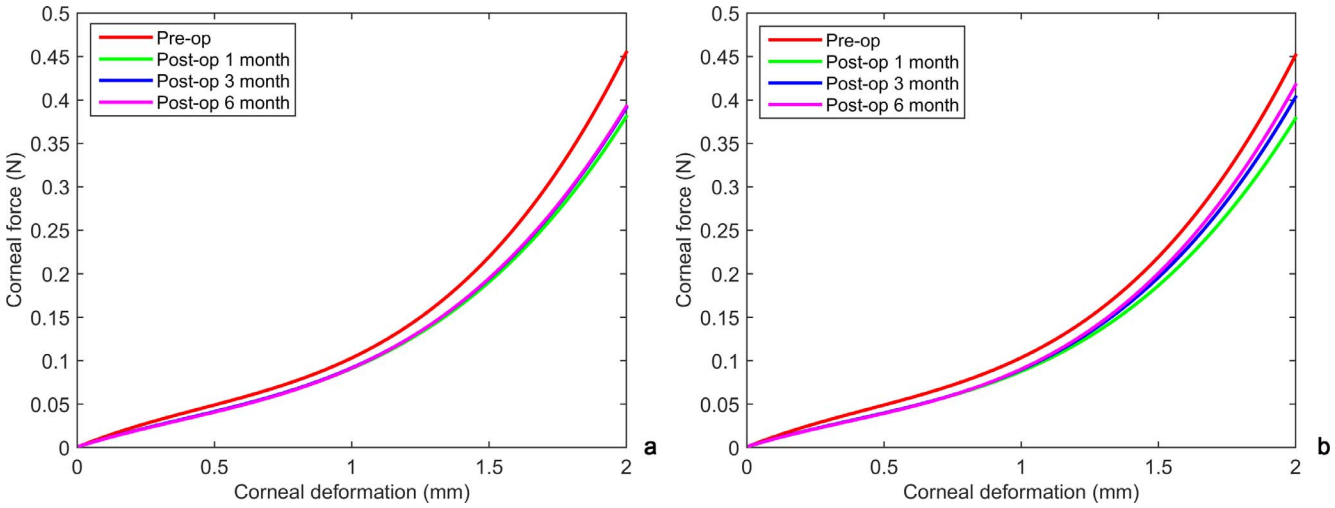

Figure 4. Mean corneal force versus corneal deformation response of LASIK (**a**) and SMILE (**b**) eyes at different time points.

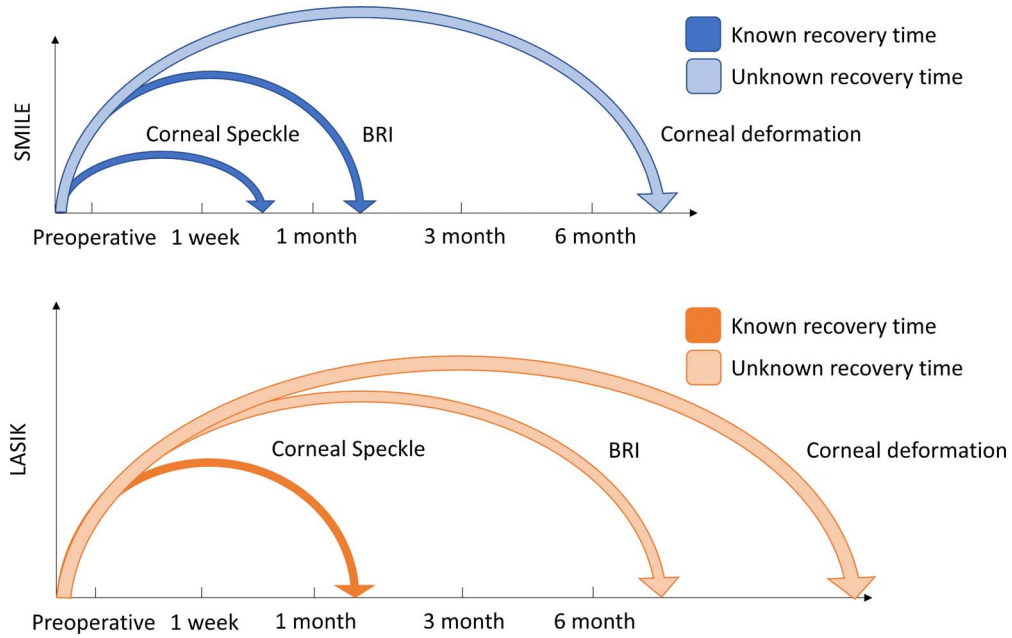

Figure 5. A schematic representation of transient changes in study parameters between SMILE and LASIK eyes.

the stroma of LASIK eyes.[28] In contrast, transient increase in high-intensity pixels in the SMILE eyes could indicate the presence of some interface fluid in the acute phase after surgery. This could lead to increased light scatter from the stroma and maybe transient complications after SMILE in a few eyes.[29,30] These transient complications may not be visible on slit lamp,[29] but OCT speckle distribution may detect these changes. There is evidence in the literature to support the speckle distribution results. SMILE generally caused less keratocyte apoptosis, less proliferation, less inflammation, and faster regeneration of nerve density than LASIK and PRK.[31–33] Interestingly, keratocyte apoptosis was observed both above and below the flap interface deep in the tissue after LASIK.[31] However, the same was localized to the lenticular interfaces only after SMILE, and the surrounding tissue showed a minimal apoptotic effect in the early phase of wound healing.[34] Thus, regional analyses of speckle distribution within the stroma could be useful in highlighting these changes since OCT is noninvasive compared to confocal microscopy. Further, speckle distribution analyses can be performed with any commercial OCT scanner since all have access to the raw (nonaveraged) OCT images. Therefore, speckle distribution may have a role in the clinic. To conclude, this study introduced a better understanding of the transient healing process after LASIK and SMILE using noninvasive imaging in patient eyes and showed a better recovery after SMILE than LASIK, biomechanically and biophysically. A longer follow-up and analyses with advanced methods, such as inverse

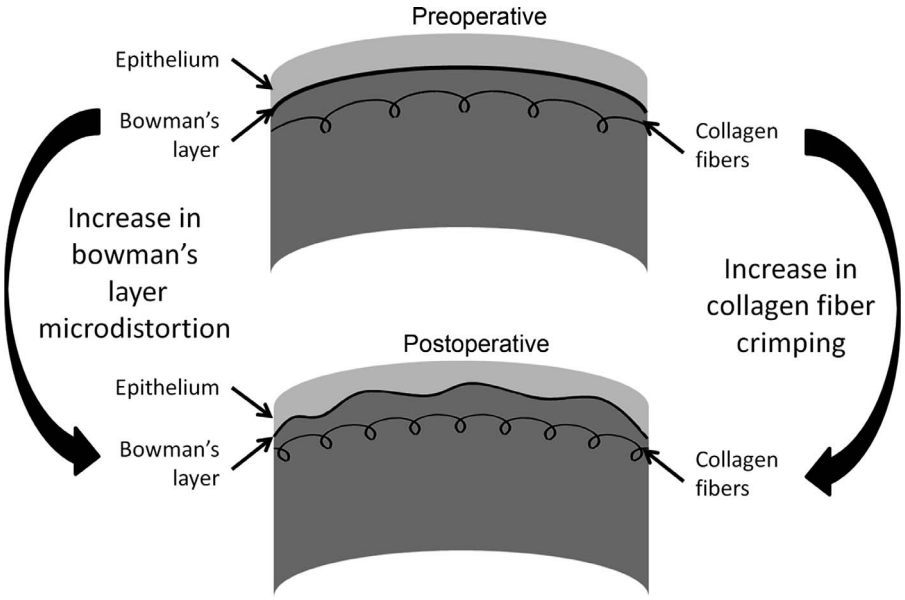

Figure 6. A schematic representation of remodeling of collagen fibers in the flap/cap region of the stroma showing the increase in microdistortions in Bowman's layer and crimping of collagen fibers.

finite element models, could reveal more interesting features of wound healing.[22]

Acknowledgments

Supported in part by a research grant from the Indo-German Science & Technology Centre (IGSTC), Government of India, and Carl Zeiss Meditec AG, Germany. The authors alone are responsible for the content and writing of the paper.

Disclosure: **R. Shetty**, None; **M. Francis**, None; **R. Shroff**, None; **N. Pahuja**, None; **P. Khamar**, None; **M. Girrish**, None; **R.M.M.A. Nuijts**, None; **A. Sinha Roy**, None

References

1. Shah R, Shah S, Sengupta S. Results of small incision lenticule extraction: all-in-one femtosecond laser refractive surgery. *J Cataract Refract Surg*. 2011;37:127–137.
2. Sekundo W, Kunert KS, Blum M. Small incision corneal refractive surgery using the small incision lenticule extraction (SMILE) procedure for the correction of myopia and myopic astigmatism: results of a 6 month prospective study. *Br J Ophthalmol*. 2011;95:335–339.
3. Zhang J, Zheng L, Zhao X, Xu Y, Chen S. Corneal biomechanics after small-incision lenticule extraction versus Q-value-guided femtosecond laser-assisted in situ keratomileusis. *J Curr Ophthalmol*. 2016;28:181–187.
4. Sefat SM, Wiltfang R, Bechmann M, Mayer WJ, Kampik A, Kook D. Evaluation of changes in human corneas after femtosecond laser-assisted LASIK and small-incision lenticule extraction (SMILE) using non-contact tonometry and ultra-high-speed camera (Corvis ST). *Curr Eye Res*. 2016;41:917–922.
5. Pedersen IB, Bak-Nielsen S, Vestergaard AH, Ivarsen A, Hjortdal J. Corneal biomechanical properties after LASIK, ReLEx flex, and ReLEx smile by Scheimpflug-based dynamic tonometry. *Graefes Arch Clin Exp Ophthalmol*. 2014;252:1329–1335.
6. Agca A, Ozgurhan EB, Demirok A, et al. Comparison of corneal hysteresis and corneal resistance factor after small incision lenticule extraction and femtosecond laser-assisted LASIK: a prospective fellow eye study. *Cont Lens Anterior Eye*. 2014;37:77–80.
7. Osman IM, Helaly HA, Abdalla M, Shousha MA. Corneal biomechanical changes in eyes with small incision lenticule extraction and laser assisted in situ keratomileusis. *BMC Ophthalmol*. 2016;16:123.
8. Wang B, Zhang Z, Naidu RK. Comparison of the change in posterior corneal elevation and corneal biomechanical parameters after small incision lenticule extraction and femtosecond laser-assisted LASIK for high myopia correction. *Cont Lens Anterior Eye*. 2016;39:191–196.
9. Wang D, Liu M, Chen Y, et al. Differences in the corneal biomechanical changes after SMILE and LASIK. *J Refract Surg*. 2014;30:702–707.
10. Wu D, Wang Y, Zhang L, Wei S, Tang X. Corneal biomechanical effects: small-incision lenticule extraction versus femtosecond laser-assisted laser in situ keratomileusis. *J Cataract Refract Surg*. 2014;40:954–962.
11. Xia L, Zhang J, Wu J, Yu K. Comparison of corneal biological healing after femtosecond LASIK and small incision lenticule extraction procedure. *Curr Eye Res*. 2016;41:1202–1208.
12. Poyales F, Garzón N, Mendicute J, et al. Corneal densitometry after photorefractive keratectomy, laser-assisted in situ keratomileusis, and small-incision lenticule extraction [published online ahead of print June 16, 2017]. *Eye (Lond)*. doi:10.1038/eye.2017.107.
13. Agca A, Cankaya KI, Yilmaz I, et al. Fellow eye comparison of nerve fiber regeneration after SMILE and femtosecond laser-assisted LASIK: a confocal microscopy study. *J Refract Surg*. 2015;31:594–598.
14. Lindenmaier AA, Conroy L, Farhat G, DaCosta RS, Flueraru C, Vitkin IA. Texture analysis of optical coherence tomography speckle for characterizing biological tissues in vivo. *Optics Lett*. 2013;38:1280–1282.
15. Jesus DA, Iskander DR. Assessment of corneal properties based on statistical modeling of OCT speckle. *Biomed Opt Express*. 2017;8:162–176.
16. Sugita M, Weatherbee A, Bizheva K, Popov I, Vitkin A. Analysis of scattering statistics and governing distribution functions in optical coherence tomography. *Biomed Opt Express*. 2016;7:2551–2564.
17. Yao P, Zhao J, Li M, Shen Y, Dong Z, Zhou X. Microdistortions in Bowman's layer following femtosecond laser small incision lenticule extraction observed by Fourier-Domain OCT. *J Refract Surg*. 2013;29:668–674.
18. Pahuja N, Shroff R, Pahanpate P, et al. Application of high resolution OCT to evaluate irregularity of Bowman's layer in asymmetric keratoconus. *J Biophotonics*. 2017;10:701–707.
19. Shroff R, Francis M, Pahuja N, Veeboy L, Shetty R, Roy AS. Quantitative evaluation of microdistortions in Bowman's layer and corneal deformation after small incision lenticule extraction. *Trans Vis Sci Tech*. 2016;5(5):12.
20. Kling S, Hafezi F. Corneal biomechanics - a review. *Ophthalmic Physiol Opt*. 2017;37:240–252.
21. Sinha Roy A, Shetty R, Kummelil MK. Keratoconus: a biomechanical perspective on loss of corneal stiffness. *Indian J Ophthalmol*. 2013;61:392–393.
22. Sinha Roy A, Kurian M, Matalia H, Shetty R. Air-puff associated quantification of non-linear biomechanical properties of the human cornea in vivo. *J Mech Behav Biomed Mater*. 2015;48:173–182.
23. Matalia J, Francis M, Tejwani S, Dudeja G, Rajappa N, Sinha Roy A. Role of age and myopia in simultaneous assessment of corneal and extraocular tissue stiffness by air-puff applanation. *J Refract Surg*. 2016;32:486–493.
24. Matalia J, Francis M, Gogri P, Panmand P, Matalia H, Sinha Roy A. Correlation of corneal biomechanical stiffness with refractive error and ocular biometry in a pediatric population. *Cornea*. 2017;36:1221–1226.
25. Pahuja N, Kumar NR, Francis M, et al. Correlation of clinical and biomechanical outcomes of accelerated crosslinking (9 mW/cm2 in 10 minutes) in keratoconus with molecular expression of ectasia-related genes. *Curr Eye Res*. 2016;41:1419–1423.
26. Grytz R, Walden AT. A computational remodeling approach to predict the physiological architecture of the collagen fibril network in corneo-scleral shells. *Biomech Model Mechanobiol*. 2010;9:225–235.
27. Yadav R, Lee KS, Rolland JP, Zavislan JM, Aquavella JV, Yoon G. Micrometer axial resolution OCT for corneal imaging. *Biomed Opt Express*. 2011;2:3037–3046.
28. Prescott P, Walden AT. Maximum likelihood estimation of the parameters of the generalized extreme-value distribution. *Biometrika*. 1980;67:723–724.
29. Agca A, Ozgurhan EB, Yildirim Y, et al. Corneal backscatter analysis by in vivo confocal microscopy: fellow eye comparison of small incision lenticule extraction and femtosecond laser-assisted LASIK. *J Ophthalmol*. 2014;2014:265012.
30. Kamiya K, Shimizu K, Igarashi A, Kobashi H. Visual and refractive outcomes of femtosecond lenticule extraction and small-incision lenticule extraction for myopia. *Am J Ophthalmol*. 2014;157:128–134.
31. Dong Z, Zhou X, Wu J, et al. Small incision lenticule extraction (SMILE) and femtosecond laser LASIK: comparison

of corneal wound healing and inflammation. *Br J Ophthalmol*. 2014;98:263–269.

32. Wei S, Wang Y, Wu D, Zu P, Zhang H, Su X. Ultrastructural changes and corneal wound healing after SMILE and PRK procedures. *Curr Eye Res*. 2016;41:1316–1325.
33. Li M, Niu L, Qin B, et al. Confocal comparison of corneal reinnervation after small incision lenticule extraction (SMILE) and femtosecond laser in situ keratomileusis (FS-LASIK). *PLoS One*. 2013;8:e81435.
34. Sekundo W. *Small Incision Lenticule Extraction (SMILE): Principles, Techniques, Complication Management, and Future Concepts*. Switzerland: Springer International Publishing; 2015:38–41.

Investigative Ophthalmology & Visual Science